

# Kinetic Modeling of Chiral Amplification and Enantioselectivity Reversal in Asymmetric Reactions

Jesús Rivera Islas and Thomas Buhse\*

Centro de Investigaciones Químicas, Universidad Autónoma del Estado de Morelos, Avenida Universidad 1001, Colonia Chamilpa, 62209 Cuernavaca, Morelos, México. Tel/Fax: +52-7773297997, e-mail: buhse@uaem.mx.

Recibido el 30 de marzo de 2007; aceptado el 18 de mayo de 2007

**Abstract:** Nonlinear effects in asymmetric synthesis and the occasionally observed reversal of the enantioselectivity of the employed catalyst are evaluated by a generalized kinetic approach. A non-autocatalytic and an autocatalytic reaction system are considered as two different prototype scenarios. It is predicted that during the course of enantioselectivity reversal in the non-autocatalytic system a gradual transition between both optically active states under loss of chiral amplification occurs while in the autocatalytic system a sharp transition under retention of chiral amplification is observed.

**Keywords:** Asymmetric synthesis, chiral amplification, nonlinear effects, organozinc additions, catalysis.

**Resumen:** Los efectos no lineales en síntesis asimétrica y la inversión de la enantioselectividad del catalizador empleado son evaluados a través de un modelado cinético generalizado. Un sistema reactivo autocatalítico y otro no autocatalítico son considerados como dos escenarios prototipos diferentes. Se predice que durante el curso de la inversión de la enantioselectividad en el sistema no autocatalítico ocurre una transición gradual entre los dos estados óptimamente activos donde la amplificación quiral decae mientras en el sistema autocatalítico ocurre una transición abrupta observándose la retención de la amplificación quiral.

**Palabras clave:** Síntesis asimétrica, amplificación quiral, efectos no lineales, adición de organozinc, catálisis.

## Introduction

Chiral amplification is characterized by the increase of optical activity during the course of an asymmetric reaction. It stands in contrast to common enantioselective synthesis where the product enantiomeric excess (*ee*) usually remains below or, at maximum, equal to the *ee* of the chiral auxiliary or initiator. It is also distinct from classical procedures of chiral enrichment such as stoichiometric resolution, conglomerate crystallization or chiral chromatography in which the increase in the *ee* goes typically along with a decrease in the amount of chiral matter as for example by the formation of *meso* species [1].

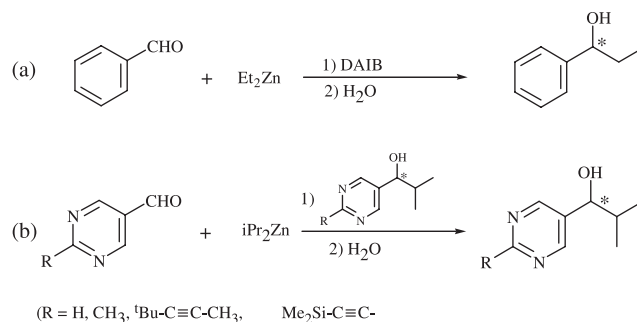
Regardless of such limitations, it was soon recognized that in specific cases of enantioselective catalysis the relation between the *ee* of the chiral auxiliary and that of the product can deviate from linearity [2-3]. Nonlinear effects in which the achievable product *ee* becomes higher than *ee* of the chiral auxiliary result in chiral amplification while the opposite case stands for chiral depletion. These effects are usually of kinetic origin and are caused by the formation of dimeric or higher-order homochiral and heterochiral species that interfere directly or indirectly with the catalytic cycle.

A variety of nonlinear effects have been found in asymmetric synthesis involving the interaction between organometallic compounds and chiral ligands to form enantioselective catalysts [4]. Noyori pioneered the addition of diorganozincs to benzaldehyde in the presence of (-)-3-*exo*-(dimethylamino)isoborneol (DAIB) yielding the chiral benzyl alcohol with a considerably higher *ee* than that of the added DAIB [5]. This type of reaction belongs to the most intriguing examples of nonlinear effects in asymmetric synthesis because it has been later extended by Soai and co-workers to a chirally autocatalytic reaction that can be driven without adding chiral

auxiliaries [6] (see Scheme 1 for the typical representation of both types of reactions).

Apart from the fundamental question for the dynamic origin of these effects, there are additional experimental observations in these systems that still lack closer kinetic understanding. Among these observations is the reversal of the enantioselectivity of the employed chiral catalysts that can occur in the presence of achiral additives as observed in organozinc additions [7,8] and other asymmetric reactions [9-11]. In such cases the chiral catalyst of one specific configuration can give rise to the two opposite enantiomeric product species when the concentration of the achiral additive is varied.

In this paper, we will present a generalized kinetic model accounting for the nonlinear relationship between the *ee* of the auxiliary and of the product in a non-autocatalytic asymmetric reaction. Introducing achiral additives, we will show that such a model can give rise to the effect of enantioselectivity rever-

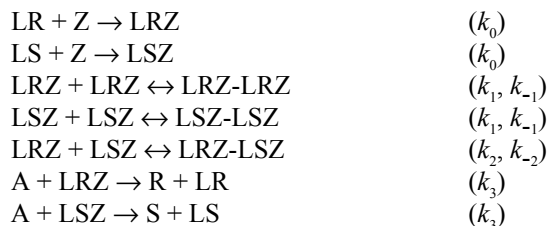


**Scheme 1.** Enantioselective addition of dialkylzinc to aldehydes: (a) Noyori-type amino-alcohol catalyzed reaction and (b) Soai-type product catalyzed reaction referring to the non-autocatalytic and autocatalytic kinetic model as presented in this article.

sal. As a continuation of our previous work [12], we will also give a further developed generalized description of enantioselectivity reversal in the Soai-type autocatalytic organozinc addition.

## Results and Discussion

After generalization, the asymmetric synthesis via organozinc additions could be expressed by the following scheme (non-autocatalytic kinetic model):

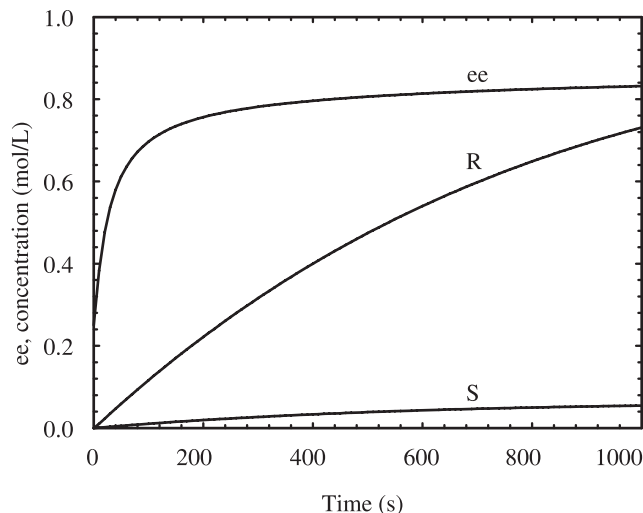


Here LR and LS stand for chiral ligands, Z for the organozinc reactant, A for the prochiral substrate and R and S for the chiral reaction products.

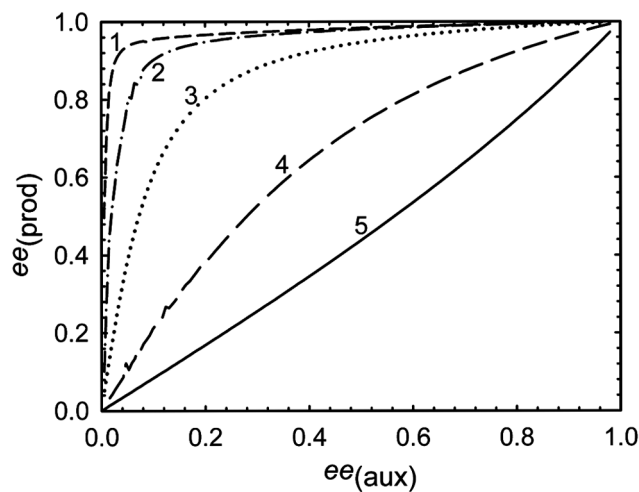
The model comprises the addition of the organozinc reactant to the chiral ligands and the subsequent dimerization of these adducts to form homochiral (LRZ-LRZ, LSZ-LSZ) and heterochiral (LRZ-LSZ) dimers where, following the mechanistic studies of Noyori and co-workers [5], the monomers exhibit the catalytic activity to form the R and S products during the reaction with A.

Figure 1 shows that the above non-autocatalytic model can give rise to a pronounced nonlinear effect in which the initial *ee* of 25% is being amplified to over 80% during the course of the reaction under constant generation of chiral matter. The magnitude of chiral amplification depends mainly on the rate parameter values. This circumstance becomes apparent in the ratio of  $k_1/k_2$ , i.e., in the difference between the rate of homo- and heterodimerization of the catalytic monomers.

Figure 2 indicates how variations in the rate constants of these two processes affect the chiral amplification strength. In order to achieve a positive nonlinear effect, the values of the involved rate parameters  $k_1$ ,  $k_{-1}$  and  $k_2$ ,  $k_{-2}$  must be in a range describing a higher stability of the heterochiral dimers over the homochiral ones, i.e.  $k_2/k_{-2} = K_{\text{HETERO}} > k_1/k_{-1} = K_{\text{HOMO}}$ . This can be readily explained by the essential need for enantiomeric cross-inhibition which is similar to the key process of chiral enrichment proceeding in conglomerate crystallizations [13]. In the present case, chiral matter composed of equal amounts of the two enantiomeric monomers LRZ and LSZ is temporarily trapped in form of a *meso* compound (LRZ-LSZ) so that the *ee* of the free monomers increases. These free monomers participate in the catalytic cycle so that consequently the chiral catalysts bear a higher *ee* than the *ee* of the initially added ligands LR and LS. This finally can result in chiral amplification if LRZ and LSZ exhibit sufficiently high stereoselectivity. For simplicity, in our modeling absolute stereoselectivity has been assumed.

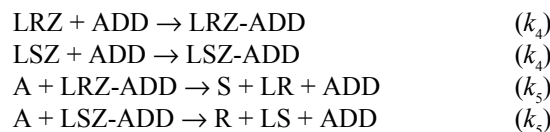


**Fig. 1.** Typical time-evolution of the R and S products and the *ee* by simulation of the non-autocatalytic kinetic model considering sufficiently high enantiomeric cross-inhibition ( $K_{\text{HETERO}} > K_{\text{HOMO}}$ ). Initial concentrations (M):  $[\text{A}] = 1$ ,  $[\text{Z}] = 2$ ,  $[\text{LR}] = 2.5 \cdot 10^{-2}$ ,  $[\text{LS}] = 1.5 \cdot 10^{-2}$  ( $ee_0 = 0.25$ ). Arbitrarily chosen parameters:  $k_0 = 0.1 \text{ M}^{-1}\text{s}^{-1}$ ,  $k_1 = 10^3 \text{ M}^{-1}\text{s}^{-1}$ ,  $k_2 = 10^5 \text{ M}^{-1}\text{s}^{-1}$ ,  $k_{-1} = k_{-2} = k_3 = 1 \text{ s}^{-1}$ .



**Fig. 2.** Product *ee* obtained by simulations of the non-autocatalytic kinetic model vs. the *ee* of the chiral auxiliary (variations in  $[\text{LS}]_0$  between zero and  $2.5 \times 10^{-2} \text{ M}$  by maintaining  $[\text{LR}] = 2.5 \cdot 10^{-2} \text{ M}$ ) showing the influence of the cross-inhibition strength on chiral amplification. Same conditions as in Fig. 1.  $K_{\text{HETERO}} : K_{\text{HOMO}} = 10000$  (curve 1,  $k_2 = 10^7 \text{ M}^{-1}\text{s}^{-1}$ ), 1000 (curve 2,  $k_2 = 10^6 \text{ M}^{-1}\text{s}^{-1}$ ), 100 (curve 3,  $k_2 = 10^5 \text{ M}^{-1}\text{s}^{-1}$ ), 10 (curve 4,  $k_2 = 10^4 \text{ M}^{-1}\text{s}^{-1}$ ), and 1 (curve 5,  $k_2 = 10^3 \text{ M}^{-1}\text{s}^{-1}$ ).

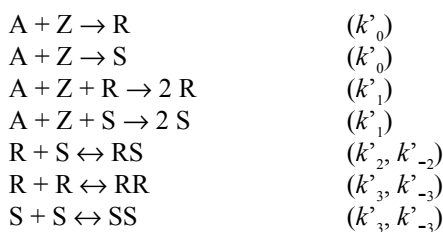
To account for the effect of enantioselectivity reversal in the presence of achiral additives, the following processes were added to the non-autocatalytic kinetic model:



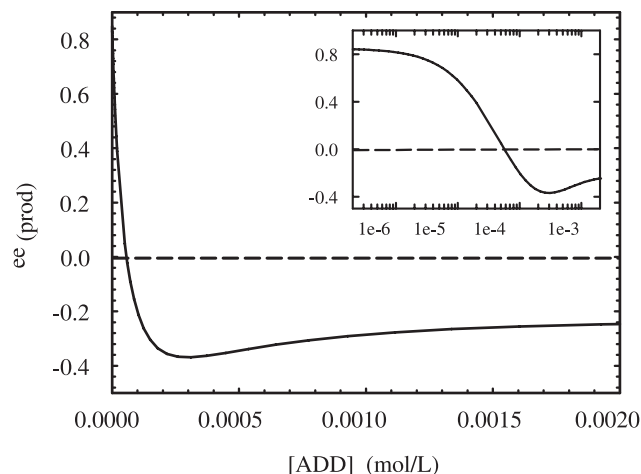
Here ADD stands for the achiral additive that was assumed to interact with the catalytic species LRZ and LSZ. Following the suggestion of Lutz *et al.* for the effect of enantioselectivity reversal in the Soai reaction [8], we assumed the formation of the new catalytic species LRZ-ADD and LSZ-ADD that promote the generation of the chiral products with opposite configuration to the implanted chiral ligands LR and LS, i.e., LRZ-ADD yields the S product and LSZ-ADD the R product. For symmetry reasons, the rate constants for the two processes involving these new catalytic species are the same. As shown in Fig. 3, this assumption can give rise to the reversal of enantioselectivity as a function of the achiral additive concentration.

The transition between the two opposite optically active states appears to occur gradually, which stands in contrast to the corresponding phenomenon observed in the autocatalytic dialkylzinc addition [8, 14]. It is also indicated that the positive nonlinear effect, which resulted in the present case in an increase of the initial *ee* from 25 to 85%, is mainly lost after the incident of enantioselectivity reversal. However, it is predicted that the *ee* goes through a quite narrow range after the reversal at which the product *ee* is still slightly higher than the initial one of the chiral ligands. However, at higher concentrations of the additive, the obtained *ee* drops below the value of the initial *ee* although always a non-racemic outcome is obtained. When the concentration of the achiral additive is very small, i.e., before the reversal occurs, the catalytic formation of the chiral product is governed by the catalytic steps ( $k_3$ ) under the retention of enantioselectivity while at higher concentrations the catalytic steps ( $k_5$ ) become dominating and promote the enantioselectivity reversal. Our modeling shows that enantioselectivity reversal in the proposed form is essentially of kinetic origin.

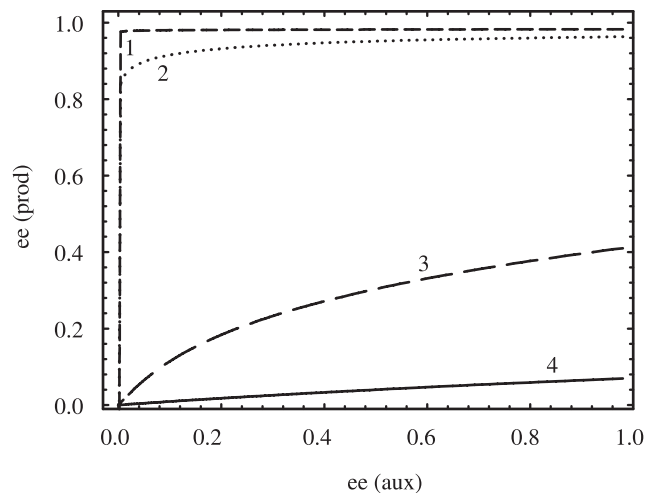
For the autocatalytic Soai-type organozinc addition, we have proposed the following minimal kinetic model that has been already confirmed to account for various experimental observations [15,16] (autocatalytic kinetic model):



Here we consider an uncatalyzed and unspecific direct formation of the R and S products from the prochiral substrate A and the organozinc reagent Z ( $k'_0$ ), a simple and not further specified description of the autocatalytic steps assuming the product monomers as catalytic species ( $k'_1$ ), and monomer-dimer equilibria ( $k'_{-2}, k''_{-2}$ ) and ( $k'_{-3}, k''_{-3}$ ) in which different rates of dimer formation for homochiral and heterochiral species is permitted. The later processes are dynamically equivalent to the steps ( $k_1, k_{-1}$ ) and ( $k_2, k_{-2}$ ) of the non-autocatalytic model and describe the mutual inhibition between the opposite enantiomers.



**Fig. 3.** Simulation of enantioselectivity reversal by the non-autocatalytic kinetic model as a function of the achiral additive (ADD) concentration. The insert shows [ADD] on a *log* scale underlining the comparatively gradual transition. Same conditions and parameters as in Fig. 1;  $k_4 = 10^5 \text{ M}^{-1}\text{s}^{-1}$  and  $k_5 = 100 \text{ M}^{-1}\text{s}^{-1}$ .



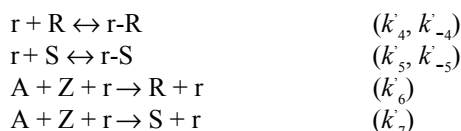
**Fig. 4.** Product *ee* obtained by simulations of the autocatalytic kinetic model vs. the *ee* of the chiral auxiliary. Initial concentrations (M): [A] = 0.2, [Z] = 0.4, [R] =  $10^{-4}$ , [S] varied between zero and  $10^{-4}$ ;  $k'_0 = 5.2 \cdot 10^{-3} \text{ M}^{-1}\text{s}^{-1}$ ,  $k'_1 = 69 \text{ M}^{-2}\text{s}^{-1}$ ,  $k'_{-2} = 0.052 \text{ s}^{-1}$ ,  $k'_3 = 4.8 \cdot 10^3 \text{ M}^{-1}\text{s}^{-1}$ ,  $k'_{-3} = 21 \text{ s}^{-1}$ . Ratio  $K_{\text{HETERO}} : K_{\text{HOMO}} = 3786$  (curve 1,  $k'_2 = 45000 \text{ M}^{-1}\text{s}^{-1}$ ), 378.6 (curve 2,  $k'_2 = 4500 \text{ M}^{-1}\text{s}^{-1}$ ), 37.9 (curve 3,  $k'_2 = 450 \text{ M}^{-1}\text{s}^{-1}$ ), and 3.8 (curve 4,  $k'_2 = 45 \text{ M}^{-1}\text{s}^{-1}$ ).

Fig. 4 shows model simulations similar to those given in Fig. 2 for the non-autocatalytic system. In contrast to the former case, the nonlinear effect appears tremendous if the ratio  $K_{\text{HETERO}} / K_{\text{HOMO}}$  is relatively high (strong mutual inhibition, lines 1 and 2). In this situation the product *ee* rises immediately to almost 100% already when the initial *ee* is extremely small or even at zero. This astonishingly pronounced scenario of chiral amplification originates from the autocatalytic nature

of the model system and, most of all, from the effect of spontaneous mirror-symmetry breaking, which is a basic characteristic of the Soai-type organozinc addition [15, 17-19]. Mirror-symmetry breaking expresses the sustained formation of significant *ee* from achiral initial conditions and can only occur in a dynamically nonlinear system [20]. On the other hand, if  $K_{\text{HETERO}}/K_{\text{HOMO}}$  becomes smaller (weaker mutual inhibition, lines 3 and 4), the nonlinear effect is suddenly lost and the product *ee* remains below the initial *ee*. The comparatively abrupt change from strong chiral amplification to even enantiomeric loss originates mainly from the transition from to a mirror-symmetry breaking to a non-mirror-symmetry breaking regime.

Recently, we have proposed a kinetic description for a particularly interesting observation of the Soai system – namely, the effect of deeply marked enantioselectivity reversal in the presence of achiral additives [12]. Specifically, the reversal has been detected in a series of reactions by simultaneously adding pairs of chiral and achiral *b*-amino alcohol catalysts that were of similar chemical structure (e.g. DMNE and DBAE) [11]. It was found that at a certain ratio of the concentrations of the chiral and achiral catalysts a sharp reversal of the enantioselectivity of the chiral catalyst took place.

Following an improved and more straight-forward kinetic approach to account for this effect, we propose the following processes being added to the basic autocatalytic model of the Soai system:



Here the additionally introduced species *r* stands typically for a pro-*R* catalyst, e.g. (1*R*,2*S*)-DMNE, which, if sufficiently concentrated, is known to direct the Soai reaction towards the *R* product. This added catalyst is considered to interact slightly with both of the Soai reaction products *R* and *S*, ( $k_4$ ,  $k_{-4}$ ) and ( $k_5$ ,  $k_{-5}$ ) as well as to display the expected biased catalytic activity in the formation of *R* and *S*, ( $k_6$ ) and ( $k_7$ ). For symmetry reasons, the given kinetic steps perform equivalent for the addition of a pro-*S* catalyst.

In the following, we will show that the consideration of only the pro-*R* catalyst (or equivalently the pro-*S* catalyst) is sufficient in our simulations to obtain the reversal of enantioselectivity. Hence the achiral additive that was present in the experimental system is not an essential ingredient in our generalized approach. The variation of the initial concentration of *r* is sufficient to drive the reaction either towards the *R* or *S* product, respectively.

The obtained enantioselectivity reversal can be understood by a competition between those processes that give rise either to the *R* product or to the *S* product in the entire reaction network. Due to the enantiomeric cross-inhibition,  $R + S \rightleftharpoons RS$  ( $k_2$ ,  $k_{-2}$ ), any process that generates *R* inhibits at the same time the formation of *S* and the same is true for the

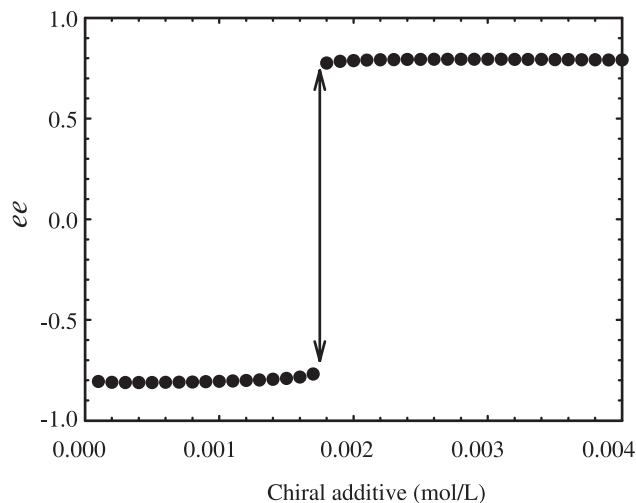


**Fig. 5.** Simulation of enantioselectivity reversal by the autocatalytic kinetic model in the presence of the chiral additive *r* (pro-*R* catalyst). Initial concentrations (M):  $[A] = 0.02$ ,  $[Z] = 0.04$ ,  $[r]$  varied between zero and 0.004;  $k_0 = 5.2 \times 10^3 \text{ M}^{-1}\text{s}^{-1}$ ,  $k_1 = 69 \text{ M}^2\text{s}^{-1}$ ,  $k_2 = 4.5 \times 10^5$ ,  $k_{-2} = 0.052 \text{ s}^{-1}$ ,  $k_3 = 4.8 \times 10^3 \text{ M}^{-1}\text{s}^{-1}$ ,  $k_{-3} = 21 \text{ s}^{-1}$ ,  $k_4 = 9.52 \times 10^3 \text{ M}^{-1}\text{s}^{-1}$ ,  $k_{-4} = 100 \text{ s}^{-1}$ ,  $k_5 = 9.48 \times 10^3 \text{ M}^{-1}\text{s}^{-1}$ ,  $k_{-5} = 100 \text{ s}^{-1}$ ,  $k_6 = 0.02375 \text{ M}^2\text{s}^{-1}$  and  $k_7 = 0.02365 \text{ M}^2\text{s}^{-1}$ .

opposite. Moreover, the *R* and *S* enantiomers become partially complexed by the interaction with *r*, ( $k_4$ ,  $k_{-4}$ ) and ( $k_5$ ,  $k_{-5}$ ). Because of diastereomeric implications, the complexes *r-R* and *r-S* are allowed to display distinct thermodynamic stabilities that can cause a bias in the concentrations of the free *R* and *S*. This happens already when the respective association rate constants differ less than  $10^{-11} \text{ M}^{-1}\text{s}^{-1}$ . Consequently, the complexation of the *R* and *S* enantiomers by *r* partially withdraws the autocatalytic species *R* and *S* from the autocatalytic cycles  $A + Z + R \rightarrow 2R$  and  $A + Z + S \rightarrow 2S$ .

If *r* shows pronounced stereoselectivity, as it does for instance the (1*R*,2*S*)-DMNE catalyst, the competition between  $k_4$  and  $k_6$  is already sufficient to give rise to the enantioselectivity reversal. In such case *R* is inhibited by the process  $r + R \leftrightarrow r - R$  but generated by  $A + Z + r \rightarrow R + r$ . As shown in Fig. 5, this delicate interplay can result in a steep transition between the two optically active states as a function of the catalyst concentration, as it has been observed in experiment by Soai and co-workers [11]

As indicated, enantioselectivity reversal takes place at a lower concentration of *r* at which the formation of the *S* product dominates while retention of the enantioselectivity is obtained at a higher concentration of *r* where the expected *R* product is formed. The steep transition between the two optically active states, as indicated by the arrow in Fig. 5, as well as the maintenance of strong chiral amplification after the reversal can be regarded as a dynamic fingerprint of the autocatalytic organozinc addition while in the non-autocatalytic reaction the enantioselectivity reversal is predicted to occur more gradually and chiral amplification is mostly lost (Fig. 3).

## Conclusion

We have presented a simplified kinetic model to rationalize the so-called nonlinear effects in asymmetric synthesis in a non-autocatalytic reaction system. We have shown that enantioselectivity reversal can occur in these systems in the presence of achiral additives that interact with the enantioselective catalysts to form new catalytic species that display reversed enantioselectivity. Hence it is supposed that enantioselectivity reversal is basically of kinetic origin. In our simulations, we have found a comparatively smooth transition from one optically active state to the other where the nonlinear effect, i.e. the chiral amplification, is mostly lost after the reversal. The prediction of this kinetic mechanism requires experimental verification, for instance by performing a series of experiments under systematic variation of the achiral additive concentration as well as monitoring the time-evolution of the *ee*.

In the case of the autocatalytic organozinc addition, respective experimental data is already available that shows a steep transition between the two optically active states during the event of enantioselectivity reversal. This steep transition stands in contrast to the smoother transition predicted for the non-autocatalytic case. We have proposed a kinetic model which is based on an interaction between the chiral additive (external catalyst) and the reaction product (internal autocatalyst) that is able to reproduce the reversal. It is supposed that the achiral additive, which is present in the experimental system, perhaps does not play an essential role for the reversal other than to 'dilute' the added external catalyst. Hence further kinetic studies are indicated, for instance by the evaluation of enantioselectivity reversal in the presence very small concentrations of the external chiral catalyst.

## Methods

The kinetic simulations were performed with the simulation-adjustment program Sa 3.3 on a personal computer as described elsewhere [15,16]. The general algorithm for the numerical integration of the differential equations was based on the semi-implicit fourth-order Runge-Kutta method with stepwise control for stiff ordinary differential equations that was sufficiently robust and reliable for nonlinear problems of the present case. Both scenarios of non-autocatalytic and autocatalytic organozinc additions were evaluated by using arbitrarily chosen but chemically realistic rate parameter values and by rigorously considering the full range of interrelated processes. In the case of the autocatalytic model system, the rate parameters  $k'_0$  to  $k'_{-3}$  have been derived from experimental data fitting as it was reported earlier [15].

## References

1. De Min, M.; Levy, G.; Micheau, J. C. *J. Chim. Phys.* **1988**, *85*, 603-619.
2. Puchot, C.; Samuel, O.; Duñach, E.; Zhao, S.; Agami, C.; Kagan, H. B. *J. Am. Chem. Soc.* **1986**, *108*, 2353-2357.
3. Kitamura, M.; Okada, S.; Noyori, R. *J. Am. Chem. Soc.* **1989**, *111*, 4028-4036.
4. Girard, C.; Kagan, H. B. *Angew. Chem. Int. Ed. Engl.* **1998**, *37*, 2922-2959.
5. Noyori, R.; Suga, S.; Oka, H.; Kitamura, M. *Chem. Rec.* **2001**, *1*, 85-100.
6. Soai, K.; Shibata, T.; Morioka, H.; Choji, K. *Nature* **1995**, *378*, 767-768.
7. Sosa-Rivadeneira, M.; Muñoz-Muñiz, O.; De Parrodi, C. A.; Quintero, L.; Juaristi, E. *J. Org. Chem.* **2003**, *68*, 2369-2375.
8. Lutz, F.; Igarashi, T.; Kawasaki, T.; Soai, K. *J. Am. Chem. Soc.* **2005**, *127*, 12206-12207.
9. Vogl, E. M.; Gröger, H.; Shibasaki, M. *Angew. Chem. Int. Ed.* **1999**, *38*, 1570-1577.
10. Walsh, P. J.; Lurain, A. E.; Balsells, J. *Chem. Rev.* **2003**, *103*, 3297-3344.
11. Ordóñez, M.; Hernández-Fernández, E.; Xahuentitlaa, J.; Cativiela, C. *Chem. Commun.* **2005**, 1336-1338.
12. Lavabre, D.; Micheau, J. C.; Rivera Islas, J.; Buhse, T. *J. Phys. Chem. A* **2007**, *111*, 281-286.
13. Thiemann, W. *Naturwissenschaften* **1982**, *69*, 123-129.
14. Lutz, F.; Sato, I.; Soai, K. *Org. Lett.* **2004**, *6*, 1613-1616.
15. Rivera Islas, J.; Lavabre, D.; Grevy, J. M.; Hernández Lamoneda, R.; Rojas Cabrera, H.; Micheau, J. C.; Buhse, T. *Proc. Natl. Acad. Sci. USA* **2005**, *102*, 13743-13748.
16. Buhse, T. *J. Mex. Chem. Soc.* **2005**, *49*, 328-335.
17. Gridnev, I. D.; Serfimov, J. M.; Quiney, H.; Brown, J. M. *Org. Biomol. Chem.* **2003**, *1*, 3811-3819.
18. Soai, K.; Sato, I.; Shibata, T.; Komiyama, S.; Hayashi, M.; Matsueda, Y.; Imamura, H.; Hayase, T.; Morioka, H.; Tabira, H.; Yamamoto, J.; Kowata, Y. *Tetrahedron: Asymmetry* **2003**, *14*, 185-188.
19. Kawasaki, T.; Suzuki, K.; Shimizu, M.; Ishikawa, K.; Soai, K. *Chirality* **2006**, *18*, 479-482.
20. Kondepudi, D. K.; Asakura, K. *Acc. Chem. Res.* **2001**, *34*, 946-954.